# CHAPTER 3

# ENHANCED ADAPTIVE WAVELET FILTER (EAWF)

This chapter discusses the basics of wavelet denoising and an Enhanced Adpative Wavelet Filter (EAWF) for the removal of speckle noise present in US images.

## 3.1 WAVELET BASED DENOISING

Figure 3.1 shows the block diagram of wavelet based denoising procedure.

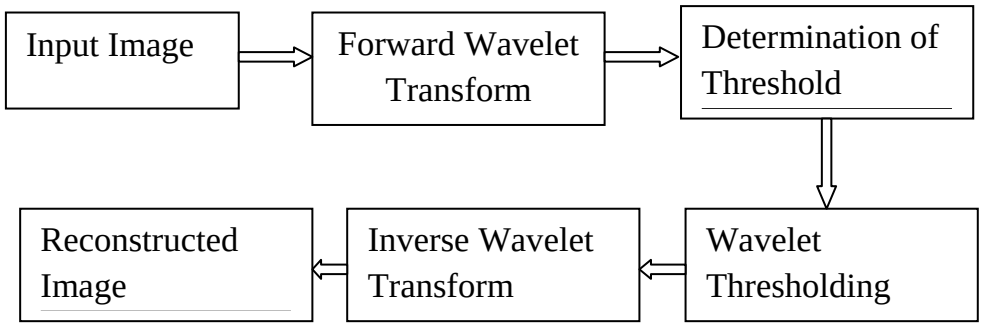


**Figure 3.1 Block diagram of wavelet based denoising**

Wavelet denoising performs the following steps:

i) taking Forward wavelet transform

ii) estimation of signal and noise variance

iii) determination of threshold

iv) shrinking the wavelet coefficients using a thresholding rule

v) reconstruction of denoised image using inverse wavelet transform

In the wavelet domain, a noise affected image is represented as a linear combination of wavelet transform of the original image and noise, as given in Equation (3.1).

$$Y(i,j) = X(i,j) + N(i,j) \tag{3.1}$$

where $Y(i,j)$ is the noise affected image, $X(i,j)$ is the noise free image and $N(i,j)$ is the noise content. A non-decimated wavelet transform decomposes the noise corrupted image into subbands to the required number of levels. Each level consists of a low frequency subband (LL) called approximation subband and three high frequency subbands (LH, HL and HH) named detail subband, with equal number of coefficients in all the levels. Let the notation for the detail coefficients is $W_D^l = \{W_D^1, W_D^2, W_D^3 .....W_D^L\}$, where $l$ denotes the resolution levels $l = \{1, 2, 3, .....L\}$ and $D$ represents the orientation of the subbands (LH, HL and HH).

Estimation of Noise Variance

Image denoising applications require the knowledge of signal and/or noise variance for the determination of threshold. As $HH^1$ subband consists of maximum high frequency coefficients, it is used for estimating the noise variance. Using the robust median estimator, it is estimated (Chang et al 2000b) as given in Equation (3.2).

$$\sigma^2 = \left( \frac{\text{Median}(|W(i,j)|)}{0.6745} \right)^2, \quad W(i,j) \in \text{subband } HH^1 \tag{3.2}$$

where $W_{ij}$ is the wavelet coefficients at location $(i,j)$.

Estimation of Signal Variance

Commonly the signal variance in denoising applications is estimated by using Maximum-A-Posteriori (MAP) or Maximum Likelihood (ML) estimate.

Generally, wavelet transformed image is of the form given in Equation (3.3).

$$Y(i, j) = X(i, j) + N(i, j) \tag{3.3}$$

Where Y(i,j) is the noisy coefficient, X(i,j) is the noise free wavelet coefficient and N(i,j) is the noise content. Hence

$$\sigma_Y^2 = \sigma_X^2 + \sigma^2 \tag{3.4}$$

$\sigma_x^2$ is the signal variance, $\sigma^2$ is the noise variance and $\sigma_Y^2$ is the variance of noise affected image and is empirically estimated as in Equation (3.5).

$$\sigma_y^2 = \frac{1}{MN} \sum_{i,=1}^{M} \sum_{j=1}^{N} W(i, j)^2 \tag{3.5}$$

where $MN$ is the length of the subband. Then the signal variance using ML estimate is obtained as in Equation (3.6).

$$\sigma_X{}^2 = \max(\sigma_Y^2 - \sigma^2, 0) \tag{3.6}$$

In the case that $\sigma^2 \geq \sigma_y^2$, $\sigma_x$ is taken to be 0, Chang et al (2000b).

## 3.2 ENHANCED ADAPTIVE WAVELET FILTER (EAWF)

EAWF is developed to enhance the performance of Qin et al (2010). Qin proposed an adaptive wavelet shrinkage method to reduce the fixed bias of soft thresholding approach using a level adaptive threshold. Determination of an adaptive threshold, making use of the local spatial features of the coefficients and the incorporation of secondary wavelet properties (intra and inter-scale dependencies) are suggested for future research by Qin et al (2010). The steps followed in the proposed denoising scheme are:

(i) performing preliminary coefficient classification

(ii) estimation of homogeneity measure based signal variance

(iii) wavelet shrinkage using thresholding function

### 3.2.1 Preliminary Clustering of Signal and Noise Coefficients

The first step in the proposed filtering approach is to determine an inter scale dependency measure to perform the preliminary coefficient classification. Preservation of edge features with removal of noise is the objective of any denoising algorithm. The key ingredient in the preservation of edges is to determine the presence of feature of interest coefficients. The classification of features of interest and noise in the wavelet domain can be done in a more flexible way due to the following properties of wavelet transformation.

- Multi resolution – it gives idea about image details existing at different levels.

- Sparsity – signal energy is concentrated only in a few large magnitude coefficients and the remaining coefficients represent noise.
- Edge detection – edge pixels are seen as large magnitude coefficients.
- Edge Clustering – in each subband, edge coefficients have a tendency to form spatially associated clusters
- Edge evolution across scales – The coefficients with high magnitude (edges), continues to exist across scales.

Owing to these facts, the dependencies of the wavelet coefficients within and across resolution scales thus give information about feature of interest (edges) and noise. The dependency measures have been used in wavelet denoising, for thresholding, determining the signal of interest and edge detection as investigated by Ge & Mirchandani (2004), Pizurica et al (2006) and Sadler & Swami (1998). Here a new measure is defined for determining the inter scale relationship among the wavelet coefficients in adjacent subbands as in Equation (3.7).

$$W^{l}(i,j) = 0 \quad \text{if} \quad \left|W^{l+1}(i,j)\right| \leq \alpha\sigma^{2} \tag{3.7}$$

where $\sigma^2$ is the noise variance and $\alpha$ is a constant and it is experimentally determined as 2. If the coefficient at coarser scale is less than the threshold, it can be considered as an insignificant coefficient and the corresponding coefficient at its finer scale is made zero. A matrix of values is derived for all the detail subbands of the wavelet decomposition, by applying Equation (3.7). The matrix thus obtained is multiplied with their corresponding detail subbands. The resultant subband is then used for estimating the parameters for threshold.

### 3.2.2 Estimation of Homogeneity Measure based Signal Variance

Several researchers have analyzed the estimation of context based signal variance for adaptive threshold determination. The context is defined through a Local Spatial Activity Measure (LSAM). In general, LSAM used in the literature are the parent coefficient magnitude as in Sendur and Selesnick (2002); the average of the (weighted) coefficient magnitudes as in Chang et al (2000a) or the local variance within a small window as in Michak et al (2004) or local regularity estimated at the corresponding position as given in Pizurica (2002) and Pizurica et al (2002). Hence it is seen from the literature that to achieve superior quality in denoising, the threshold value is to be selected considering the subband statistics along with local spatial context.

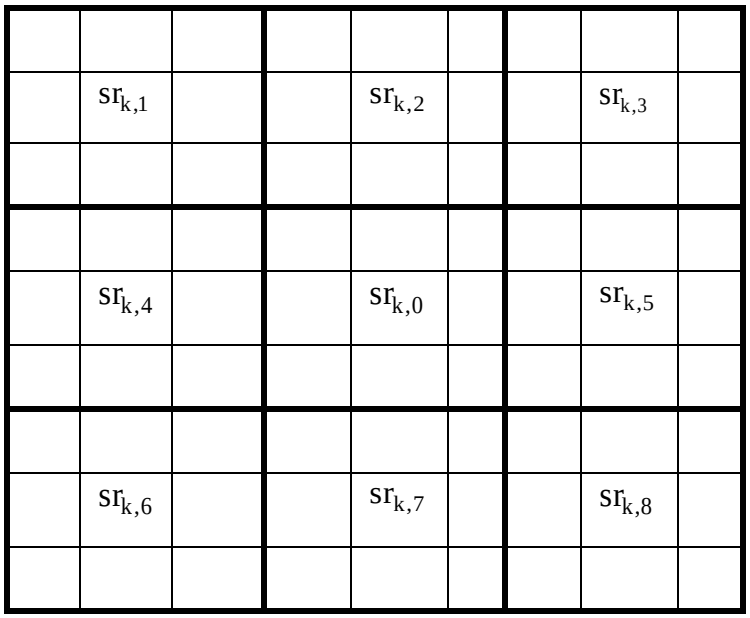


**Figure 3.2 A square region R (9x9) and its sub regions (3x3) in a subband**

This section discusses a simple method of signal variance estimation for determination of adaptive threshold. LSAM in the present approach is a homogeneity measure and is derived by exploiting the inter scale correlation of the coefficients. The procedure for determining the

homogeneity measure is a modified method of Eom & Kim (2004). Their approach is modified by exploiting the inter scale dependencies in determining the homogeneity measure. The procedure starts with dividing a subband in to a region R and further into sub regions as shown in Figure 3.2.

A square region R of size 9x9 is considered in the subband $W_D^l(i,j)$ at resolution level $l$ and orientation $D$. The region is then divided into sub regions $sr_{k,0}, sr_{k,1}, sr_{k,2} \ldots\ldots sr_{k,S-1}$, $k$ representing the pixel location $(i,j)$. The sub regions are partitioned in such a way that they are non-overlapping $(sr_{k,x} \cap sr_{k,y}; x \neq y)$ and their union generates the region $R(\cup_s sr_{k,s} = R)$. The coefficient under consideration $W(i,j)$ is at the centre $sr_{k,0}$ and at the centre of R. The region and their associated sub regions are shown in Figure 3.2. Homogeneity measure is defined as the normalized difference of variances between the sub region containing the coefficient under consideration and all the other sub regions in the region R. Here a region merging procedure is followed. Starting from the sub region $sr_{k,0}$, which contains the coefficient to be processed, merging continues until the homogeneity of variance is achieved. The equation for finding homogeneity measure is given as in Equation (3.8),

$$h_{k,s} = \frac{\left|\sigma_{k,s}^2 - \sigma_{k,0}^2\right|}{\sigma_{k,0}^2},\ s = 0,1,2 \ldots S-1 \tag{3.8}$$

where $\sigma_{k,s}^2$ is the local variance of the region $sr_{k,s}$. The variance of the sub regions is calculated locally as in Equation (3.9)

$$\sigma_{k,s}^2 = \left( \frac{1}{|n(k)|} \sum_{W(i,j) \in n(k)} W^2(i,j) \right)_+ \tag{3.9}$$

where n(k) is the neighborhood, $|n(k)|$ is the cardinality of the neighborhood and $W(i,j)$ is the coefficient in the neighborhood. The homogeneity measure $h_{k,s}$ is then compared with some specific threshold, to determine the shape of the window. Here a level adaptive threshold is used to determine the homogeneous variance given by Equation (3.10)

$$t_k = C.2^{(L-l)}, l = 1,2.....L \tag{3.10}$$

where C is the scaling parameter and is empirically determined to be equal to 0.1 and $l = 0$ is the finest scale of decomposition and $l = L$ is the coarsest scale of decomposition. If the homogeneity measures of the sub regions are less than the specified threshold then that sub region is included in the window. A binary matrix is defined as in Equation (3.11) to indicate whether the variance $\sigma^2_{k,s}$ is homogeneous with $\sigma^2_{k,0}$ or not.

$$v_{k,s} = \begin{cases} 1 & h_{k,s} < t_k \\ 0 & \text{otherwise} \end{cases} \tag{3.11}$$

The signal variance is then estimated as in Equation (3.12) ,

$$\sigma^2_x = \left( \frac{\sum_{s=0}^{S-1} \sigma^2_{k,s} v_{k,s}}{\sum_{s=0}^{S-1} v_{k,s}} - \sigma^2_n \right)_+ \tag{3.12}$$

Thus the new signal variance is estimated using a locally adaptive window of neighborhoods using homogeneous measure.

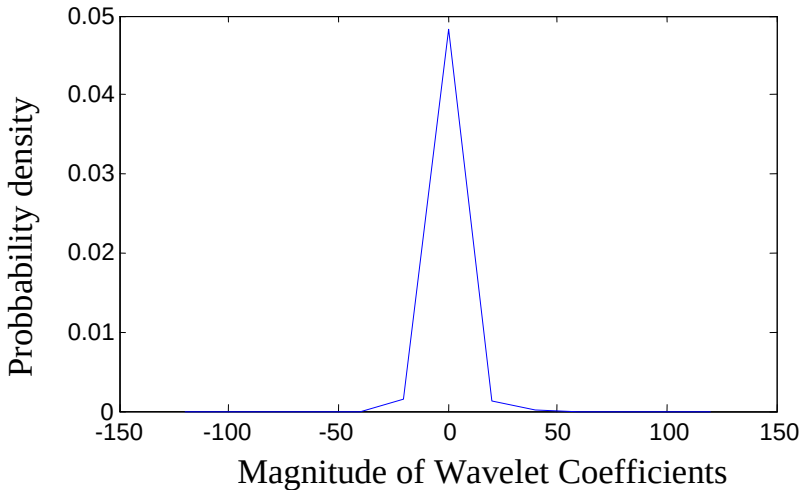


**Figure 3.3 Histogram pdf of $HH^1$ subband**

Figure 3.3 shows the pdf of the histogram of $HH^1$ subband and Figure 3.4 shows the pdf generated with ML and homogeneity measure based variances. It is seen from the figures that the pdf generated with homogeneity measure based variance model the coefficients comparatively better than the ML estimate.

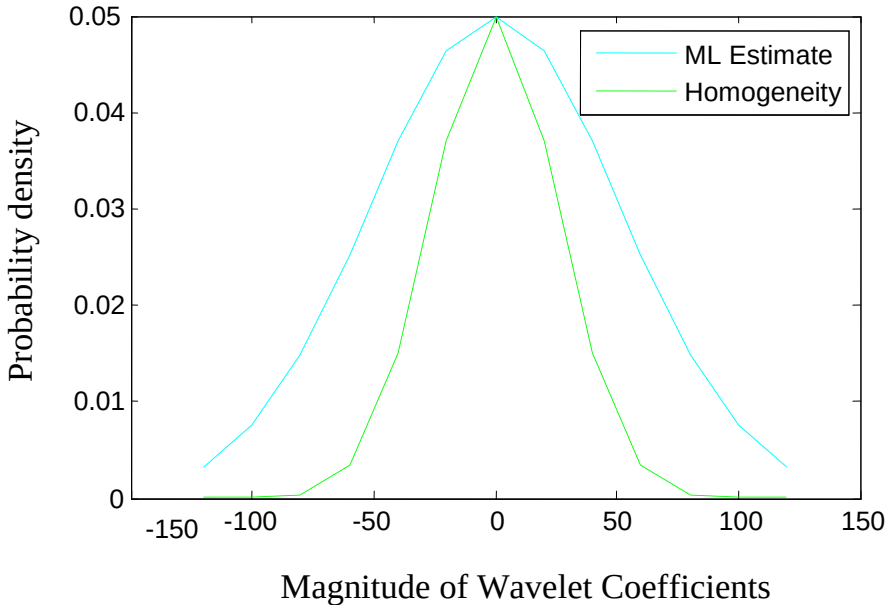


**Figure 3.4 Comparison of pdfs' generated with ML and homogeneity measure based variances for $HH^1$ subband**

### 3.2.3 Threshold Determination

The selection of the best possible threshold is a critical task in the development of denoising filters, as it is an important factor in determining the quality of denoising. Among the various shrinkage techniques discussed in section (1.5), Bayes threshold, employed a threshold that is optimal in terms of mean squared error. Bayes shrink is developed to be subband adaptive and is optimized with regard to the marginal subband statistics.

In this approach, the Bayes threshold is refined with a subband adaptation parameter, to further improve the adaptivity of the threshold. The proposed adaptive threshold ($\lambda_{MB}$) is defined as in Equation (3.13).

$$\lambda_{MB} = \beta_l T_B \tag{3.13}$$

where $\beta_l$ is the subband adaptation parameter and $T_B$ is the Bayes threshold given by Equations (3.14) and (3.15) respectively.

$$\beta_l = \sqrt{\frac{\log M}{2 * 2^l}} \tag{3.14}$$

$$T_B = \frac{\sigma^2}{\sigma_x} \tag{3.15}$$

where M is the size of the subband and l is the current level of decomposition. The subband adaptation parameter $\beta$ provides a better adaptability to the threshold at various levels of decomposition. $\sigma^2$ is the noise variance estimated using Equation (3.2) and $\sigma_x$ is the signal standard deviation estimated using Equation (3.6).

### 3.2.4 Adaptive Thresholding Function

The adaptive thresholding function of Qin et al (2010) is defined as in Equation (3.16)

$$\hat{W}_{i,j} = \operatorname{sgn}(W(i,j))\left(|W(i,j)| - \left(1 - \exp\left(\frac{-m}{|w^2(i,j) - \lambda^2_{MB}|}\right)\right)\lambda_{MB}\right) \qquad |W(i,j)| \geq \lambda_{MB}$$

$$= 0 \qquad |W(i,j)| < \lambda_{MB} \tag{3.16}$$

where $\hat{W}(i,j)$ is the denoised coefficient, $W(i,j)$ is the noisy wavelet coefficient, $\lambda_{MB}$ is the subband adaptive threshold as defined in Equation (3.13) and m is a positive constant. If $m \to \infty$, Equation (3.16) approaches the soft thresholding function and if $m \to 0$, it approaches hard thresholding function. By changing the value of m, effective thresholding operation is achieved. The comparison of hard, soft and the proposed threshold functions are shown in Figure 3.5.

As seen from the graph, the fixed bias of soft thresholding function is reduced in Qin et al (2010) approach. It is close to hard shrinkage, have smaller bias than the soft shrinkage for large coefficients. It is continuous like soft shrinkage. The reduction in fixed bias reduces the difference between the original and the reconstructed coefficients, which improved the performance of the filter and in visual quality.

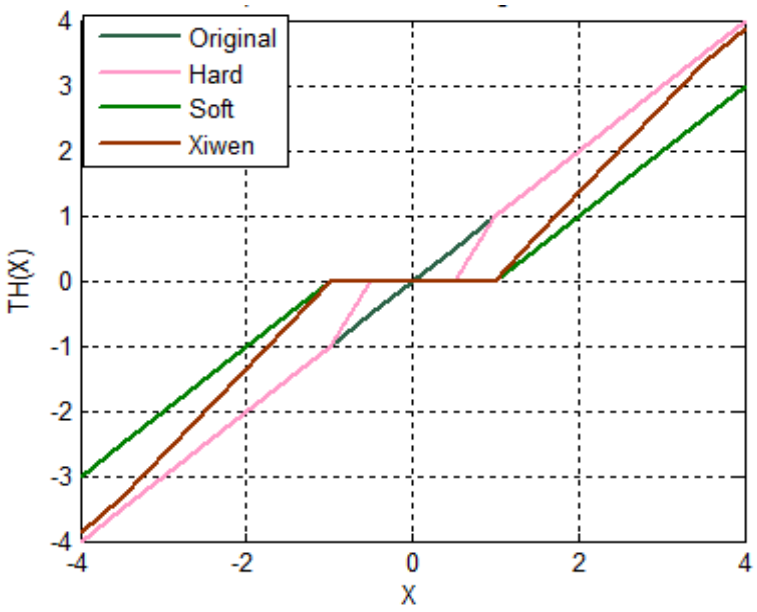


**Figure 3.5 Comparison of thresholding functions**

### 3.2.5 Summary of the Denoising Algorithm for EAWF

The stepwise implementation of the above discussed procedure is given below:

Step 1: Decompose the input noisy image to L levels by applying stationary wavelet transform.

Step 2: Compute the noise variance using Equation (3.2)

Step 3: Compute the inter scale dependency measure for each of the detail subbands LH, HL and HH using Equation (3.7)

Step 4: Multiply each of the detail subbands by the corresponding measure computed

Step 6: Compute the measure of homogeneity using Equations (3.8) to (3.11)

Step 7: Estimate the signal variance as in Equation (3.12)

Step 8: Compute the threshold using Equations (3.13) to (3.15)

Step 9: Apply the adaptive thresholding function in Equation (3.16) to estimate the noise free coefficients

Step10: Take inverse wavelet transform to reconstruct the image

## 3.3 RESULTS AND DISCUSSION

The experimental set up consists of intel i3 processor with 4GB RAM. MATLAB version 2009b is used for simulation. The image data base used comprises of 230 clinical US images of size 512 x 512. The images were collected from the data base of Edapal Hospital, Kerala and Aadharsh Scans, Erode. The US images are recorded as they are displayed in the ultrasound monitor after logarithmic transformation. For the in-vivo case (B-Mode displayed images), quantitative evaluation is difficult because of the absence of reference (speckle free) image. So, for quantitative evaluation, artificially speckled images were simulated for two cases: (i) for a synthetic phantom image and (ii) real US image free from noise, in which the natural speckle was previously suppressed.

Artificial speckle is introduced using MATLAB simulation as,

$$Y = \text{imnoise}(X, \text{'speckle'}, v) \tag{3.17}$$

where X is the original image and v is the noise variance. Speckle noise with variances 0.01, 0.04, 0.08 and 0.1 are introduced into the images. The performance of the proposed system is compared with standard speckle filters like Frost, Kuan and Lee Filters, Soft Thresholding and Qin et al (2010). Quantitative performance is measured with parameters like PSNR, MSE, SSIM, ENL and EPI. Figure 3.6 to Figure 3.8 show the sample clinical ultrasound images used for testing the present and the proposed algorithms in the following chapters. The decomposition level is set as two for the images in all the proposed approaches.

**Figure 3.6 Clinical US image1**

**Figure 3.7 Clinical US image2**

**Figure 3.8 Clinical US image3**

The simulated phantom image shown in Figure 3.9(a) is used to analyze the performance of the algorithm. The size of the phantom image is 256 x 256. Figure 3.9(b) depicts the phantom image corrupted with an artificial speckle of variance 0.1. The comparisons of visual quality of synthetic phantom image for various filters are shown in Figure 3.9. The results of standard speckle filters are shown from Figure 3.9(c) to Figure 3.9(e). It is seen that the output images are smoothed out and the contrast and hence the edges around the circles are not clearly visualized. The visual quality of soft thresholding in Figure 3.9(f) shows a slightly improved edge performance. Qin et al (2010) approach in Figure 3.9(g) reduces the noise much better but with edges blurred. The EAWF approach shows a better image quality compared to the other approaches as seen in Figure 3.9(h).

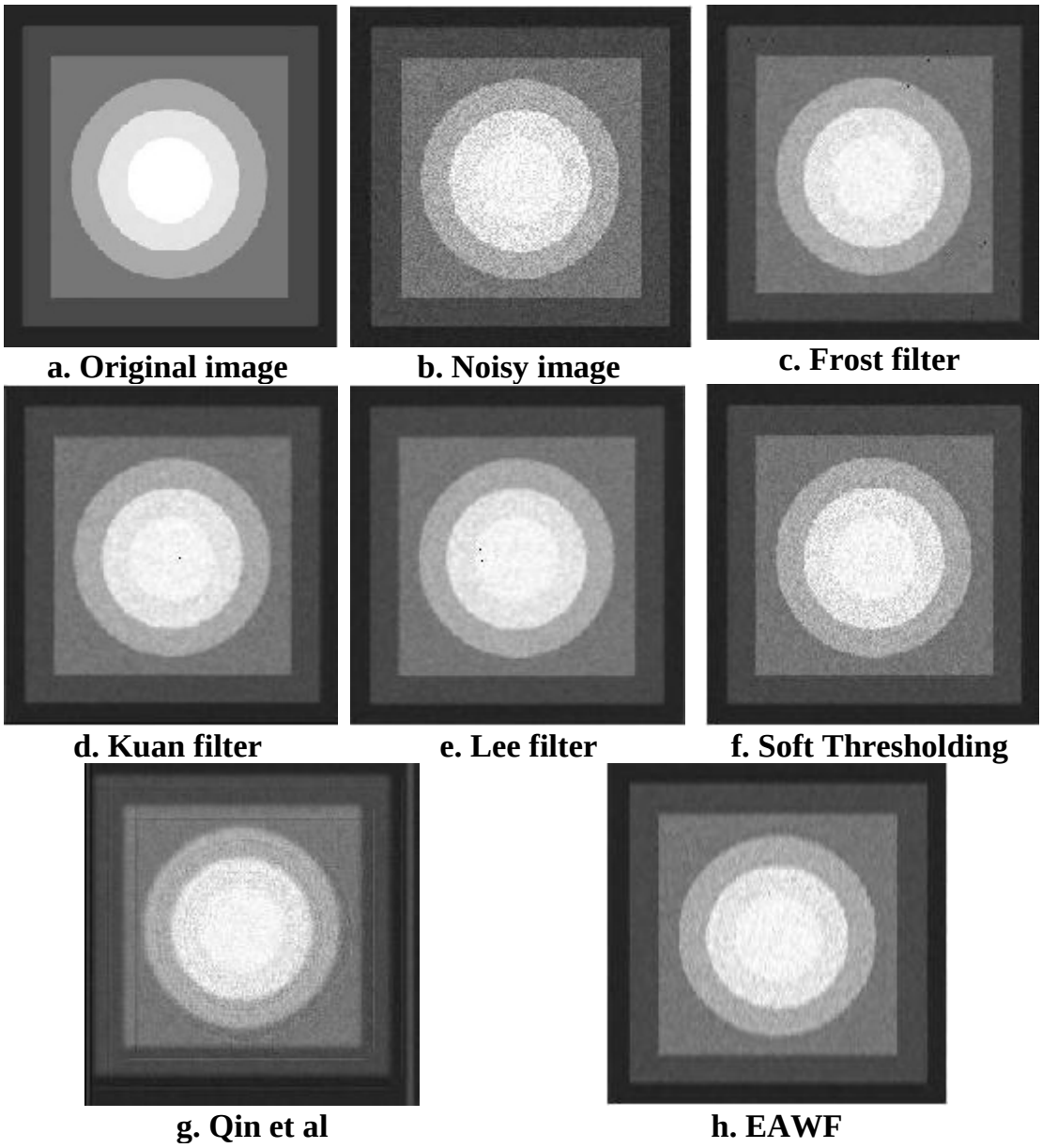

**a. Original image** **b. Noisy image** **c. Frost filter**

**d. Kuan filter** **e. Lee filter** **f. Soft Thresholding**

**g. Qin et al** **h. EAWF**

**Figure 3.9 Visual quality comparison of EAWF with various filters for synthetic phantom image**

The clinical ultrasound image shown in Figure 3.6 is tested for various noise variances and the results of denoising performance for various methods based on quantitative measure are presented in Table 3.1. The proposed algorithm is tested with different wavelet basis functions like coiflet, daubechies, symlets, haar and biorthogonal wavelets and Table 3.2 presents the comparison of performance metrics.

**Table 3.1 Performance comparison of EAWF for different noise variances and filters**

| $\sigma^2$ | Noisy | Frost | Kuan | Lee | Soft Threshold | Qin | EAWF |
|---|---|---|---|---|---|---|---|
| | **Peak Signal to Noise Ratio** | | | | | | |
| **0.01** | 34.9435 | 38.6438 | 39.8387 | 39.7923 | 36.2507 | 40.4068 | **41.8515** |
| **0.04** | 31.4191 | 34.0636 | 35.5479 | 35.5193 | 33.1247 | 36.0805 | **38.4214** |
| **0.08** | 30.4078 | 31.8946 | 32.9930 | 32.8841 | 32.0909 | 34.4780 | **36.4853** |
| **0.1** | 30.1131 | 31.2677 | 32.0888 | 32.0758 | 31.7935 | 34.0053 | **35.7670** |
| | **Mean Square Error** | | | | | | |
| **0.01** | 20.8321 | 8.8859 | 6.7485 | 6.8211 | 15.4175 | 5.9210 | **4.2455** |
| **0.04** | 46.8998 | 25.5104 | 18.1254 | 18.2455 | 31.6673 | 16.0335 | **9.3528** |
| **0.08** | 59.1965 | 42.0362 | 32.6425 | 33.4712 | 40.1782 | 23.1889 | **14.6068** |
| **0.1** | 63.3536 | 48.5639 | 40.1979 | 40.3180 | 43.0259 | 25.8553 | **17.2337** |
| | **Structural Similarity Index Measure** | | | | | | |
| **0.01** | 0.9663 | 0.9804 | 0.9819 | 0.9820 | 0.9666 | 0.9822 | **0.9848** |
| **0.04** | 0.8882 | 0.9451 | 0.9512 | 0.9515 | 0.9135 | 0.9461 | **0.9608** |
| **0.08** | 0.8104 | 0.9023 | 0.9145 | 0.9124 | 0.8559 | 0.9068 | **0.9346** |
| **0.1** | 0.7815 | 0.8798 | 0.8944 | 0.8938 | 0.8311 | 0.8913 | **0.9210** |
| | **Equivalent Number of Looks** | | | | | | |
| **0.01** | 1.6661 | 1.7021 | 1.6975 | 1.6994 | 1.6419 | 1.7094 | **1.7114** |
| **0.04** | 1.5483 | 1.6716 | 1.6844 | 1.6848 | 1.5643 | 1.6865 | **1.7125** |
| **0.08** | 1.4127 | 1.6304 | 1.6648 | 1.6636 | 1.4767 | 1.6631 | **1.7081** |
| **0.1** | 1.3606 | 1.6065 | 1.6564 | 1.6593 | 1.4347 | 1.6495 | **1.7013** |
| | **Edge Preservation Index** | | | | | | |
| **0.01** | 0.3274 | 0.2622 | 0.2244 | 0.2213 | 0.3486 | 0.5470 | **0.5766** |
| **0.04** | 0.1722 | 0.1552 | 0.1646 | 0.1628 | 0.1759 | 0.2837 | **0.4285** |
| **0.08** | 0.1239 | 0.1085 | 0.1312 | 0.1262 | 0.1221 | 0.1966 | **0.3598** |
| **0.1** | 0.1114 | 0.0974 | 0.1100 | 0.1121 | 0.1072 | 0.1763 | **0.3308** |

Table 3.1 shows results simulated using db4 wavelet filter. From Table 3.2, it is seen that Coiflet2 yields high PSNR. But compared with the other performance indices like SSIM and EPI, db4 gives better result. As preservation of edge features along with noise removal is the key objective, db4 wavelet is chosen in this experiment.

**Table 3.2 Comparison of performance metrics of EAWF for different wavelets**

| Wavelets / Metrics | db4 | bior1.1 | haar | sym2 | coief2 |
|---|---|---|---|---|---|
| **PSNR** | 41.8515 | 37.7204 | 40.1741 | 44.0661 | **49.2271** |
| **MSE** | 4.2455 | 10.9910 | 6.2470 | 2.5496 | **0.7782** |
| **SSIM** | **0.9848** | 0.2818 | 0.9820 | 0.4500 | 0.6970 |
| **ENL** | 1.7114 | 1.8556 | 1.7193 | 1.7931 | 1.7788 |
| **EPI** | **0.5766** | 0.0503 | 0.4324 | 0.0566 | 0.2618 |

From the quantitative performance comparison in Table 3.1, it is seen that the spatial domain filters like Frost, Kuan and Lee are good in removing speckle noise but lack in the preservation of edges and fine details as evident from their EPI measure. The soft thresholding approach in column 6 of Table 3.1 shows improved edge preservation compared with standard speckle filters.

It is obvious from Table 3.1 that on an average, PSNR of EAWF is increased by 4.82dB compared with soft thresholding and 1.89dB compared with Qin et al (2010). MSE is reduced on an average by 35.08% compared to Qin et al (2010). SSIM measure assesses the preservation of structural information on the denoised output. The typical value of SSIM is in the range between 0 and 1 and a value 1 represents structurally identical images. The value of SSIM for EAWF is improved compared to the existing approaches, ths indicating good structural preservation. A large value of ENL represents a good quality image and its value is higher in EAWF than in the other existing approaches considered.

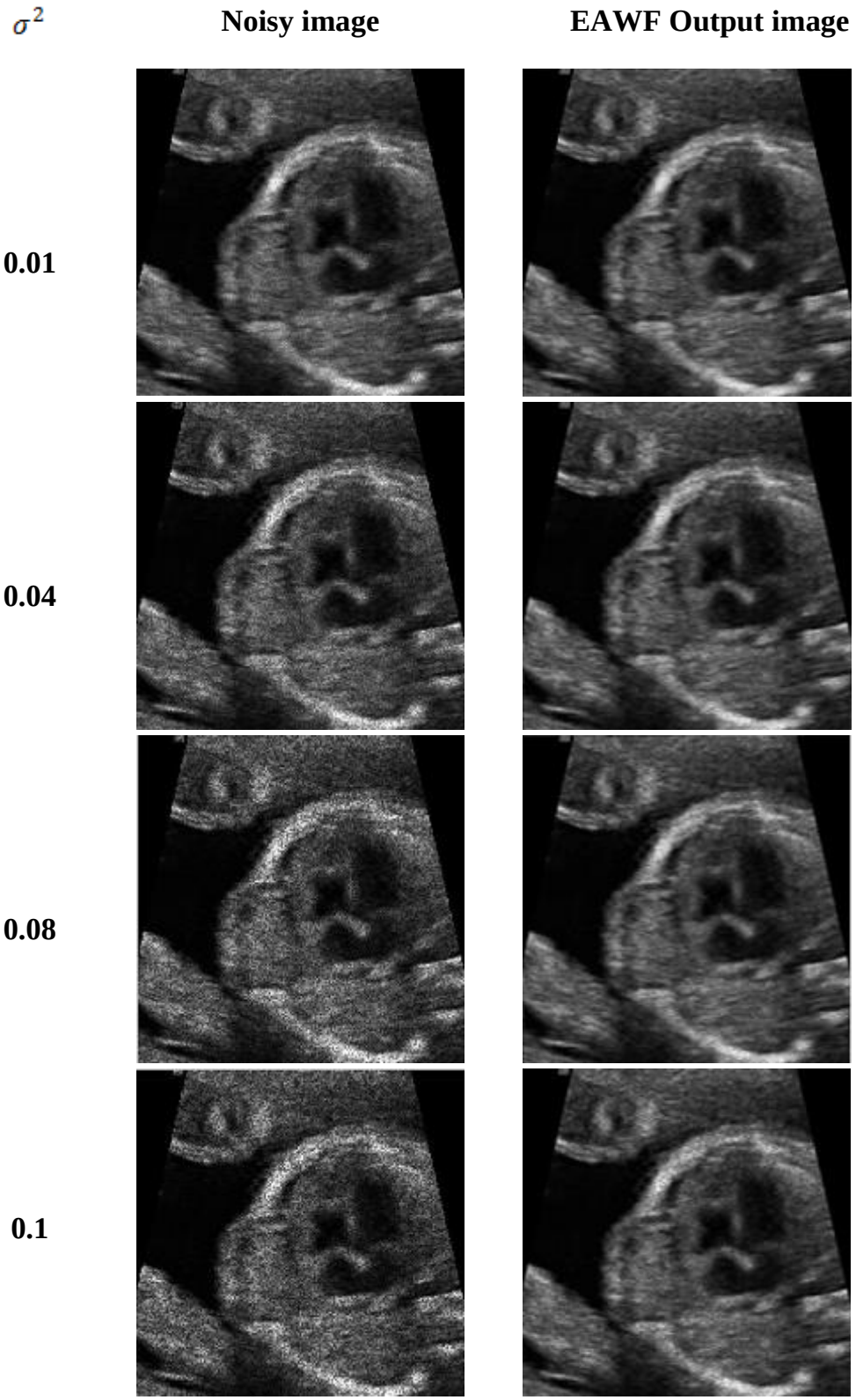


**Figure 3.10 Comparison of visual quality of EAWF for US image1 for different noise variances**

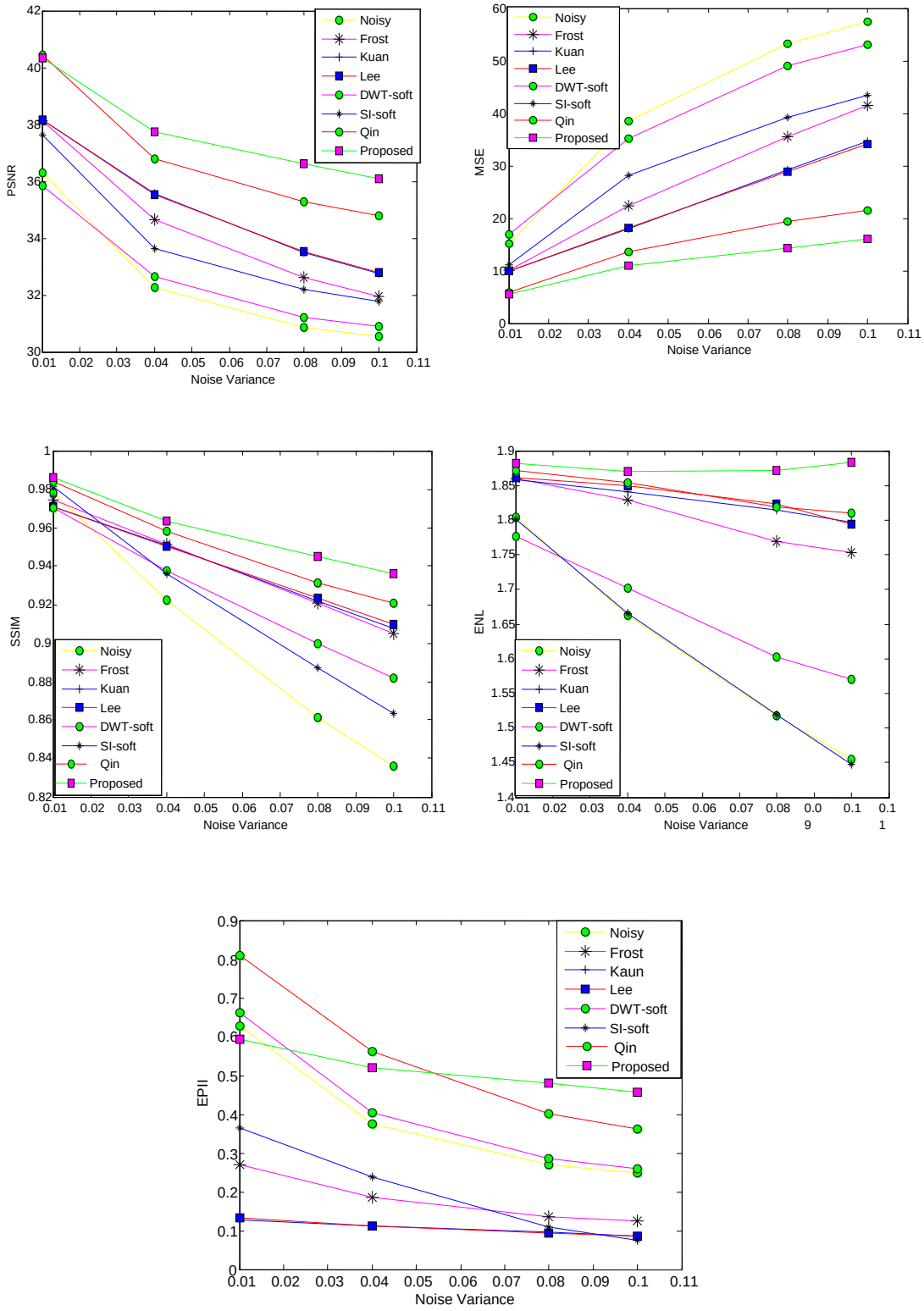


**Figure 3.11 Graphical analysis of various performance measures of EAWF for US image 2**

To enrich the result, one more parameter is also measured ( i. e.) EPI which gives the preservation of important image details in the denoised output. The maximum value of EPI should be unity. This measure is also seen to have improved and better for EAWF than the existing filtering schemes. It is improved by 32.75% compared with Qin et al (2010) on an average. For high noise variance level of 0.1, the results show a better improvement than at low (0.01) variance. The incorporation of correlation of wavelet coefficients in the determination of parameters for the threshold, thus improved the threshold selection. Hence the performance of EAWF is improved compared to Soft thresholding and Qin approaches. Also it aided in retaining the significant features of the images as reflected by the EPI index.

For the clinicians, visual quality is more important along with other performance improvement. So, the qualitative performance of EAWF is verified with visual quality comparisons of US images for different noise variances and with various filtering approaches. Figure 3.10 compares the visual quality of EAWF for US image1, for various noise variances (Column 1). The second column of Figure 3.10 shows the noisy images and the third column, their corresponding denoised outputs. The visual quality of the output images of EAWF is good even at high noise variance level of 0.1. The performance of EAWF is verified with US image2 and the comparison of various performance measures are shown via graphical analysis in Figure 3.11. From this comparison it is evident that the EAWF method shows an improvement in measures like PSNR, MSE, SSIM and ENL. In EPI, it is low for low noise variance (0.01) and seen to be improved for high variances.

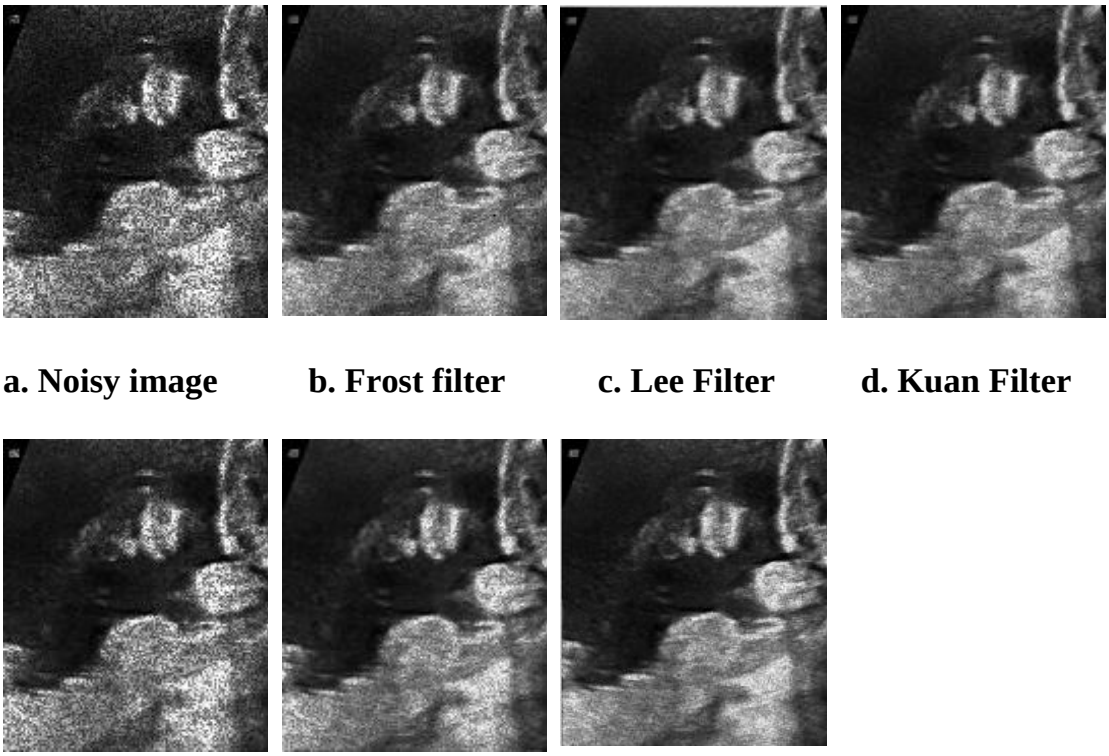

**a. Noisy image** **b. Frost filter** **c. Lee Filter** **d. Kuan Filter**

**e. Soft Thresholding** **f. Qin et al** **g. EAWF**

**Figure 3.12 Comparison of visual quality of EAWF with existing filters for US image 3**

The visual quality enhancement of EAWF is compared with various filter outputs for US image3. Figure 3.12 shows the visual quality of EAWF compared with some of the existing filter for a noise variance 0.1, for US image 3. It is seen from Figure 3.12 that for Lee filter in Figure 3.12(c), noise removal is better than Kuan Filter shown in Figure 3.12(d) and Frost filter in Figure 3.12 (b). The noise is still present in soft thresholding approach. From Figure 3.12 (g) good visual quality and improved contrast are seen in EAWF than in the other wavelet based and standard speckle approaches. Thus EAWF gives a better performance for both synthetic phantom and the clinical ultrasound images.

It is seen from the results that the edge detail preservation has increased to a small extent in EAWF. This is due to the reason that LSAM obtained through a comparison of variances in a sub-region and hence the local statistics of a pixel could not be estimated accurately. Hence, the variance estimation requires a more efficient LSAM for better threshold selection. Also, there exists still a constant bias between the original and reconstructed coefficients as seen from Figure 3.5. The number of zero valued coefficients in the reconstructed output of Equation (3.16) can be reduced by processing the low magnitude coefficients. Hence these two facts require the modification in thresholding function.

## 3.4 SUMMARY

This chapter discussed an enhanced adaptive wavelet filter with homogeneity measure based variance estimation approach. The local statistics of the coefficients in a subband are estimated via homogeneity measure as local spatial adaptivity measure. It provided the local spatial information of the coefficients and aided in the determination of adaptive threshold. The incorporation of inter scale relation in homogeneity measure estimation improved the context selection. This is evident from the improved values of PSNR and EPI measures.